

# Hidden hyperchaos and electronic circuit application in a 5D self-exciting homopolar disc dynamo

Zhouchao Wei, Irene Moroz, J. C. Sprott, Akif Akgul, and Wei Zhang

Citation: *Chaos* **27**, 033101 (2017); doi: 10.1063/1.4977417

View online: <http://dx.doi.org/10.1063/1.4977417>

View Table of Contents: <http://aip.scitation.org/toc/cha/27/3>

Published by the [American Institute of Physics](#)

---

---

Welcome to a

Smarter Search 

PHYSICS  
TODAY

with the redesigned  
*Physics Today Buyer's Guide*

Find the tools you're looking for today!

# Hidden hyperchaos and electronic circuit application in a 5D self-exciting homopolar disc dynamo

Zhouchao Wei,<sup>1,2,3,4,a)</sup> Irene Moroz,<sup>3</sup> J. C. Sprott,<sup>5</sup> Akif Akgul,<sup>6</sup> and Wei Zhang<sup>4</sup>

<sup>1</sup>*School of Mathematics and Physics, China University of Geosciences, Wuhan 430074, China*

<sup>2</sup>*Guangxi Colleges and Universities Key Laboratory of Complex System Optimization and Big Data Processing, Yulin Normal University, Yulin 537000, China*

<sup>3</sup>*Mathematical Institute, University of Oxford, Oxford OX2 6GG, England*

<sup>4</sup>*College of Mechanical Engineering, Beijing University of Technology, Beijing 100124, China*

<sup>5</sup>*Department of Physics, University of Wisconsin - Madison, Madison, Wisconsin 53706, USA*

<sup>6</sup>*Department of Electrical and Electronic Engineering, Faculty of Technology, Sakarya University, Sakarya 54050, Turkey*

(Received 21 December 2016; accepted 13 February 2017; published online 27 February 2017)

We report on the finding of hidden hyperchaos in a 5D extension to a known 3D self-exciting homopolar disc dynamo. The hidden hyperchaos is identified through three positive Lyapunov exponents under the condition that the proposed model has just two stable equilibrium states in certain regions of parameter space. The new 5D hyperchaotic self-exciting homopolar disc dynamo has multiple attractors including point attractors, limit cycles, quasi-periodic dynamics, hidden chaos or hyperchaos, as well as coexisting attractors. We use numerical integrations to create the phase plane trajectories, produce bifurcation diagram, and compute Lyapunov exponents to verify the hidden attractors. Because no unstable equilibria exist in two parameter regions, the system has a multistability and six kinds of complex dynamic behaviors. To the best of our knowledge, this feature has not been previously reported in any other high-dimensional system. Moreover, the 5D hyperchaotic system has been simulated using a specially designed electronic circuit and viewed on an oscilloscope, thereby confirming the results of the numerical integrations. Both Matlab and the oscilloscope outputs produce similar phase portraits. Such implementations in real time represent a new type of hidden attractor with important consequences for engineering applications.

*Published by AIP Publishing.* [<http://dx.doi.org/10.1063/1.4977417>]

**In a series of papers, Leonov *et al.* have shown multistability to be related to hidden attractors, whose basins of attraction contain no neighborhoods of any equilibrium, and cannot be determined by conventional methods. After the idea of hidden attractor was coined, and the first one was found in Chua's circuit, hidden attractors have received much attention. A key matter is how to identify systems with hidden attractors. Such knowledge, including how to determine the properties of hidden attractors, increase the chances that a given system remains on the most desirable attractor, thereby avoiding the risk of sudden transitions to undesirable dynamics. We present typical examples of hidden attractors, review their characteristics, and also discuss numerical methods which enable hidden attractors to be located. The results obtained expand the knowledge of hidden hyperchaos and its potential use in higher-dimension dynamical systems.**

## I. INTRODUCTION

For the past few decades, chaos and its control have been extensively studied. For 3D autonomous systems with smooth quadratic nonlinearities, Sprott used computer search techniques to identify nineteen systems exhibiting chaotic dynamics,

but with a maximum of three equilibria.<sup>1</sup> Multistability is a feature in many nonlinear dynamical models, ranging from the geophysical fluid dynamics (such as the climate and marine ecosystems) to models of finance in economics, together with engineering applications. Multistability depends on the choice of initial conditions, as well as on small changes in parameters, so that a sudden transition can occur to a different attractor.<sup>2</sup>

The current paper is concerned with the multistability and hyperchaos in a new 5D system, which extends a 3D model for a self-exciting dynamo.<sup>3</sup> Recent studies of hyperchaos in 4D, 5D, or 6D autonomous systems have mostly focused on the generation of hyperchaos with *at least one unstable equilibrium*; hyperchaotic attractors with two positive Lyapunov exponents (LEs) in 4D;<sup>4–7</sup> hyperchaotic attractors with three positive Lyapunov exponents in 5D;<sup>8–10</sup> and hyperchaotic attractors with four positive Lyapunov exponents in 6D.<sup>11</sup> Such attractors are called “self-excited” and are easily found by choosing an initial condition on the unstable manifold in the vicinity of the unstable equilibrium. Therefore, they are overwhelmingly the most common type discussed in Refs. 12–15.

Recently, a new type of attractor called a “hidden attractor,” that does not intersect with the neighborhood of any fixed point, has been a topic of discussion.<sup>16–23</sup> There has been growing interest in some unusual attractors for 3D or 4D autonomous quadratic systems including ones with no

<sup>a)</sup>Electronic mail: weizhouchao@163.com

equilibrium,<sup>24–28</sup> a single non-hyperbolic equilibrium,<sup>29</sup> stable equilibria,<sup>30–37</sup> a line of equilibria,<sup>38,39</sup> and with coexisting attractors.<sup>40–42</sup> Complex hidden dynamical behaviors (such as hyperchaos) in high-dimensional systems are not yet well understood. This provides an interesting new field of research into multistability and hidden hyperchaotic attractors.<sup>2,43,44</sup> It is therefore of interest to ascertain whether 5D autonomous systems exist that have a hidden hyperchaos with three positive Lyapunov exponents. Such systems are hard to identify because there is no systematic procedure to choose initial conditions and parameter values except by systematic but laborious numerical searches.

The investigation of hidden hyperchaotic attractors in 5D autonomous systems also has significant practical applications. Because of its inherent unpredictability, higher-dimensional hyperchaotic systems are important in investigations of control and synchronization in electronic circuits, as well as in encryption, etc., “Self-excited” hyperchaotic attractors no longer satisfy this need in secure communication and circuit implementation. Therefore, it is necessary albeit difficult to find and study the properties of new  $n$ -D systems that exhibit hidden hyperchaos and have  $n - 2$  positive Lyapunov exponents, where  $n > 4$ .<sup>15</sup>

Identification and location of coexisting attractors and their basins of attraction as parameters vary is crucial for understanding the behaviour of nonlinear systems. This becomes more difficult for hidden or rare states. Some methods are discussed in Ref. 43. Here we report on hidden hyperchaotic attractors with no unstable equilibria but with three positive Lyapunov exponents in a 5D self-exciting homopolar disc dynamo. Our hope is that this study will feed into more studies of 5D systems with quadratic nonlinearities, and so identify the geometrical characteristics of lower-dimensional chaotic and hyperchaotic attractors.

The paper is structured as follows: In Section II, we introduce the new 5D self-exciting homopolar disc dynamo and discuss the existence of equilibrium solutions. In Section III, hidden chaotic attractors, hidden hyperchaotic attractors, and multistability are shown and discussed. In Section IV, a re-scaled version of the 5D system is incorporated into an electronic circuit and viewed on an oscilloscope and observed in real-time. Section V summarizes the results and provides concluding remarks.

## II. 5D HYPERCHAOTIC SELF-EXCITING HOMOPOLAR DISC DYNAMO

Hidden attractors can be obtained by carefully choosing parameters and initial conditions in 3D or 4D systems. Here, we consider the case  $n = 5$  with attractors that are not “self-excited” and thus cannot be found by means of the local unstable manifold.<sup>43</sup> Any novel 5D system of significance, which exhibits hyperchaos, should satisfy at least one of the two criteria: (1) The system should model an important aspect of nature and provide insights into the problem; (2) the system should exhibit previously unobserved dynamics.

To obtain unusual hidden hyperchaotic attractors in an autonomous system, we demand the following conditions: (i) The proposed system has a small number of quadratic

nonlinearities; (ii) It has either no or only stable equilibria so that all attractors are hidden; (iii) It exhibits hidden hyperchaos with three positive Lyapunov exponents.

Idealized models of dynamo action have been extensively investigated in the literature as a way of understanding the generation of magnetic fields and their reversals in the Earth, the Sun, and other astrophysical bodies. In order to consider a segmentation of the disk, leaving the possibility of azimuthal currents to exclude the magnetic field, Moffatt proposed a heuristic model of the disk dynamo of Edward Bullard<sup>45–47</sup> taking into account the field exclusion process necessary to satisfy the Alfvén theorem of flux conservation<sup>3</sup>

$$\begin{cases} \dot{x} = r(y - x), \\ \dot{y} = mx - (1 + m)y + xz, \\ \dot{z} = g(1 + mx^2 - (1 + m)xy). \end{cases} \quad (1)$$

Here,  $x(t)$  and  $y(t)$  are the non-dimensional magnetic fluxes associated with the radial and azimuthal currents, respectively, while  $z(t)$  is the dimensionless angular velocity of the disc. The dot denotes differentiation with respect to re-scaled time, and  $g$ ,  $r$ , and  $m$  are positive constants which depend on the inductances and the electrical resistance of the dynamo.

In the present paper, by modifying the characteristics of the segmented disc dynamo (1), hidden chaotic or hyperchaotic spiral attractors have been observed numerically under special initial conditions with two symmetric stable node-foci. This leads to the interesting and striking observation of multiple attractors involving coexisting point attractors, limit cycles, or coexisting chaotic spiral attractors for a broad range of parameters. As in many nonlinear dynamical systems, the occurrence of multiple attractors implies the existence of multistability in the self-exciting dynamo, with the long-term behavior being fundamentally different depending on which basin of attraction, the initial conditions belong.

Motivated by the above ideals, we augment the existing dynamo model (1) with the addition of two state variables  $u$  and  $v$  to obtain the 5D autonomous system

$$\begin{cases} \dot{x} = r(y - x) + u, \\ \dot{y} = -(1 + m)y + xz - v, \\ \dot{z} = g(1 + mx^2 - (1 + m)xy), \\ \dot{u} = 2(1 + m)u + xz - k_1x, \\ \dot{v} = -mv + k_2y, \end{cases} \quad (2)$$

where  $r$ ,  $m$ , and  $g$  are positive parameters, and  $k_1$ ,  $k_2$  are control parameters. System (2) is invariant under the transformation  $(x, y, z, u, v) \rightarrow (-x, -y, z, -u, -v)$ , i.e., it has a rotational symmetry around the  $z$ -axis. Because the divergence of the flow in (2) is  $1 - r$ , system (2) is dissipative and its phase space volume contracts along a trajectory when  $r > 1$ .

Now in order to get the hidden hyperchaos with three positive Lyapunov exponents, we can exclude some parameter sets that cannot make system (2) show bounded chaotic solutions.

**Theorem 2.1.** Consider the five-parameter family of system (2) with two real parameters  $l_1, l_2$ . If parameters  $(r, g) \in (0, +\infty) \times (0, +\infty)$  and  $m, k_1, k_2, l_1, l_2$  satisfy

$$\begin{aligned}
 m &= -2 + l_1 + \frac{1}{l_2} > 0, \\
 k_1 &= \frac{l_1(-2 + l_2(2 - l_1 + r))}{l_2}, \\
 k_2 &= \frac{3 - l_2(3 + l_1(-2 + r))}{l_2^2}, \quad l_1 < 2 + 2m, \quad (3)
 \end{aligned}$$

then (2) has no bounded chaotic or hyperchaotic solutions.

**Proof.** From system (2) with real parameters  $l_1, l_2$ , we can form

$$\begin{aligned}
 \dot{y} - \dot{u} + l_1\dot{x} + l_2\dot{v} \\
 = (-1 + k_2l_2 - m + l_1r)y + (-2 + l_1 - 2m)u \\
 + (k_1 - l_1r)x + (-1 - l_2m)v. \quad (4)
 \end{aligned}$$

Under assumptions (3), Eq. (4) becomes

$$\dot{y} - \dot{u} + l_1\dot{x} + l_2\dot{v} = p(y - u + l_1x + l_2v), \quad (5)$$

whose integral is

$$y(t) + u(t) + l_1x(t) + l_2v(t) = \alpha e^{(2-l_1+2m)t},$$

where  $\alpha$  is an arbitrary constant. Hence system (2) is not chaotic because at least one of  $y(t), u(t), l_1x(t), l_2v(t)$  is not bounded when  $l_1 < 2 + 2m$ . The proof is complete.

To analyze system (2), we find its equilibria for  $a, m, g$  positive and  $k_1, k_2 \in R$ . Let

$$\begin{aligned}
 r(y - x) + u &= 0, \quad -y(1 + m) + xz - v = 0, \\
 -g(1 + m)xy + g + mgx^2 &= 0, \\
 2(1 + m)u + xz - k_1x &= 0, \quad k_2y - mv = 0. \quad (6)
 \end{aligned}$$

From the first, second, fourth, and fifth equations in (6), introducing  $\Delta_1 = k_1 - 2(1 + m)r$ ,  $\Delta_2 = k_2 - m(1 + m)(2r - 1)$ , when  $\Delta_2 \neq 0$  we find that

$$\begin{aligned}
 y &= \frac{mx\Delta_1}{\Delta_2}, \quad z = \frac{(k_2 + m + m^2)\Delta_1}{\Delta_2}, \\
 u &= \frac{(k_2 + m(1 - k_1 + m))rx}{\Delta_2}, \quad v = -\frac{k_2x\Delta_1}{\Delta_2}.
 \end{aligned}$$

Combining the third equation with (7), we obtain

$$x^2 = \frac{k_2 - m(1 + m)(2r - 1)}{m(k_1(1 + m) + (1 + m)(m + 2r) - k_2)}. \quad (7)$$

Therefore, we obtain the following results:

- (i) It is impossible for system (2) to have only one equilibrium.
- (ii) System (2) has no equilibria when  $k_2 = m(1 + m)(2r - 1)$  or  $(k_2 - m(1 + m)(2r - 1))(k_2 - k_1(1 + m) + (1 + m)(m + 2r)) > 0$ .
- (iii) System (2) has only two equilibria when  $(k_2 - m(1 + m)(2r - 1))(k_2 - k_1(1 + m) + (1 + m)(m + 2r)) < 0$ .

This result suggests where to look for hidden hyperchaotic attractors.

### III. HIDDEN ATTRACTORS AND MULTISTABILITY

Multistability, namely, the coexistence of different attractors, is a feature of many nonlinear systems and has recently been studied.<sup>23,35</sup> Multistability shows the richness of potential stable states to which a nonlinear system can evolve, gives greater versatility of the dynamics, and offers flexibility in applications such as image processing. We investigate whether such multistability occurs in higher-dimensional systems such as those that exhibit hidden hyperchaos.

To locate the hidden attractors, we need to choose parameters for which system (2) has either no equilibria or only stable equilibria. If system (2) has two equilibria  $E_{1,2}$ , they will be symmetric about the  $z$ -axis and will share the same characteristics. Therefore, we only consider the stability of equilibrium  $E_1(x_0, y_0, z_0, u_0, v_0)$ , where

$$x_0 = \sqrt{\frac{k_2 - m(1 + m)(2r - 1)}{m(k_1(1 + m) + (1 + m)(m + 2r) - k_2)}}.$$

Perturbing system (2) about the equilibrium  $E_1$ , and neglecting nonlinear terms give the quintic characteristic equation

$$\lambda^5 + \delta_1\lambda^4 + \delta_2\lambda^3 + \delta_3\lambda^2 + \delta_4\lambda + \delta_5 = 0, \quad (8)$$

where the expression for  $\delta_i (i = 1, 2, 3, 4, 5)$  is too large to print and thus is not shown here. The Routh-Hurwitz criterion provides conditions for the real parts of all the eigenvalues  $\lambda$  to be negative, namely, if and only if

$$\begin{aligned}
 \Delta_1 = \delta_1 > 0, \quad \Delta_2 = \begin{vmatrix} \delta_1 & \delta_3 \\ 1 & \delta_2 \end{vmatrix} > 0, \\
 \Delta_3 = \begin{vmatrix} \delta_1 & \delta_3 & \delta_5 \\ 1 & \delta_2 & \delta_4 \\ 0 & \delta_1 & \delta_3 \end{vmatrix} > 0, \quad \Delta_4 = \begin{vmatrix} \delta_1 & \delta_3 & \delta_5 & 0 \\ 1 & \delta_2 & \delta_4 & 0 \\ 0 & \delta_1 & \delta_3 & \delta_5 \\ 0 & \delta_1 & \delta_2 & \delta_4 \end{vmatrix} > 0, \\
 \delta_5 > 0. \quad (9)
 \end{aligned}$$

To simplify, we consider only the effect of the parameters  $r$  and  $k_1$  and set the other parameters  $m = 0.04, g = 140.6, k_2 = 12$ . Therefore, with condition (9) and complex calculations,  $E_{1,2}$  are both asymptotically stable if  $r$  and  $k_1$  lie in the yellow regions of Fig. 1, giving a further clue for where to look for hidden hyperchaotic attractors.

#### A. Hidden attractors with two stable equilibria

An important feature of the system is the existence of hidden hyperchaos for a range of parameters in asymptotically stable regions of  $E_{1,2}$  (Fig. 1). Hidden hyperchaos can occur for the choice  $m = 0.04, g = 140.6, k_2 = 12$ , and  $r = 7, k_1 = 34$ , for which the Lyapunov exponents<sup>48-50</sup> are (0.9616, 0.5477, 0.1425, 0.0000, -7.6518). They can be obtained from a standard Gram-Schmidt reorthonormalization procedure, using a Jacobian matrix. The Lyapunov exponents (LEs) we calculate are independent of initial conditions provided they are in the basin of the attractor. The LE is a running average of the local LEs along the orbit and so any point that is visited by the orbit is like taking a new

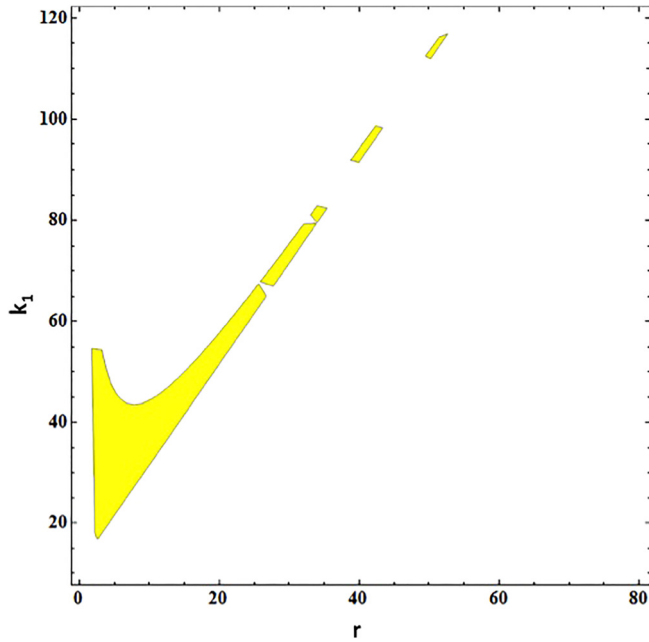


FIG. 1. The equilibria  $E_{1,2}$  of system (2) are asymptotically stable in the yellow regions.

initial condition. Although there is an infinity of unstable periodic orbits on the attractor, they form a set of measure zero and so are easily avoided as initial starting points. The Kaplan-Yorke dimension<sup>33,51,52</sup> is  $D_{KY} = 4.2159$ . The projections of the hyperchaotic attractor onto various planes are shown in Fig. 2.

To examine the robustness of the hyperchaos and show evidence of multistability, the dynamics of system (2) was investigated in the range  $3 < r < 8$  with  $k_1 = 34$  in Fig. 3 where the equilibria  $E_{1,2}$  are stable. The figure shows three

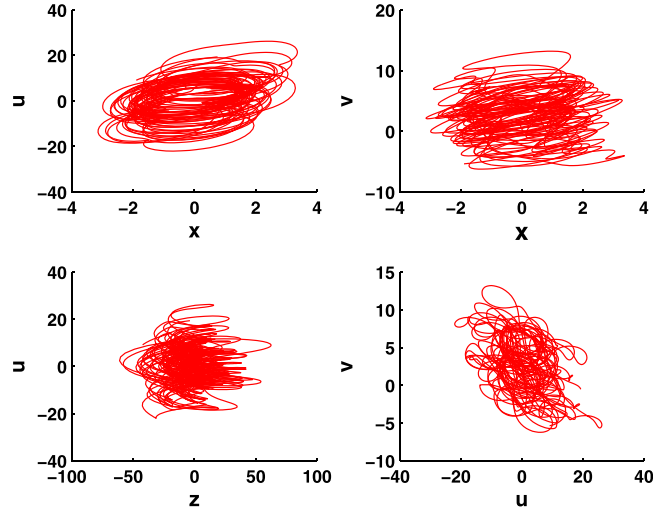


FIG. 2. Hidden hyperchaotic attractor of system (2) with parameters  $m = 0.04$ ,  $g = 140.6$ ,  $k_1 = 34$ ,  $k_2 = 12$  and  $r = 7$  and initial condition  $(0.05, -0.5, 0.1, -1, 2)$ .

choices of initial conditions. In the left panel, the initial conditions are kept constant at  $(0.05, -0.5, 0.1, -1, 2)$ , while in the middle panel,  $r$  is increased without reinitializing, and in the right panel, it is decreased without reinitializing. The figure clearly shows chaotic and hyperchaotic regions (two or three positive LEs), quasiperiodicity (where  $D_{KY} = 2$ ) with periodic windows (limit cycles) and hidden attractors as well as hysteresis. The complicated structure at small  $r$  in the left panel is a result of the initial conditions falling into a region where the attractor basins are strongly intertwined as will be illustrated later. In addition, every time a basin boundary is crossed, there is an infinitely long transient, and that the boundary is crossed countless times for small values of  $r$ .

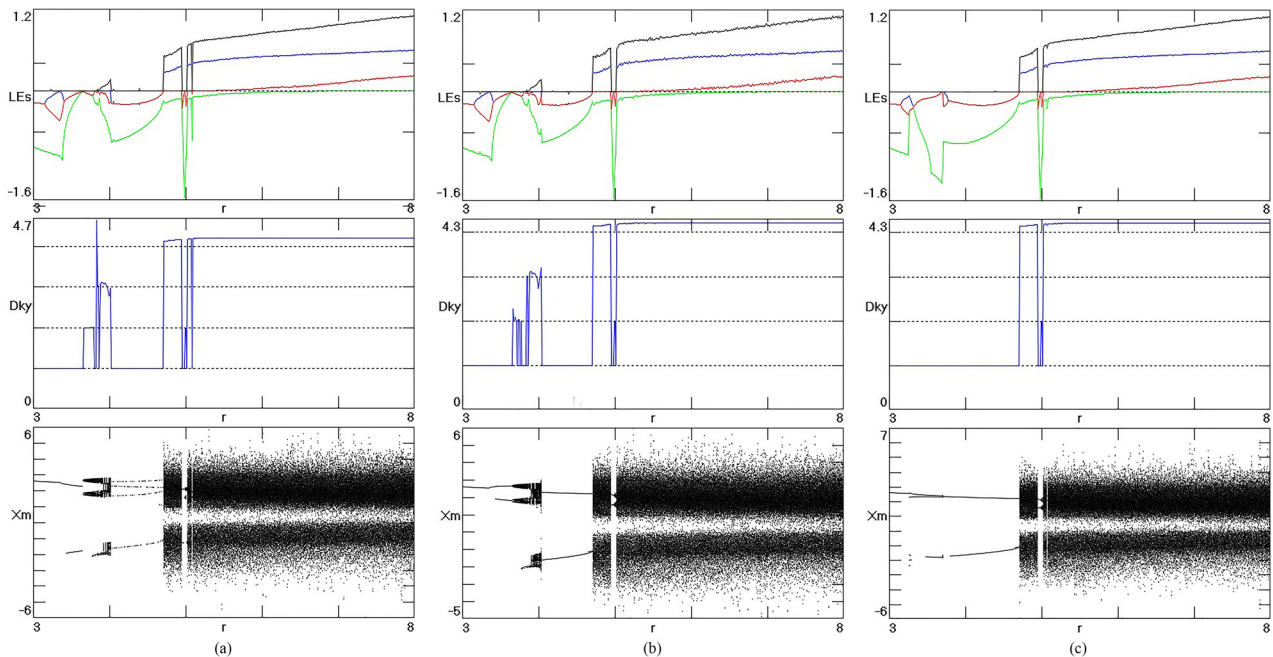


FIG. 3. The first four Lyapunov exponents (the fifth is large and negative), Kaplan-Yorke dimension and bifurcation diagrams of system (2) versus parameters  $m = 0.04$ ,  $g = 140.6$ ,  $k_1 = 34$ ,  $k_2 = 12$ : Left: fixed initial condition  $(0.05, -0.5, 0.1, -1, 2)$ ; Middle: the varied initial condition for increasing  $r$  from 3 to 8; Right: the varied initial condition for decreasing  $r$  from 8 to 3.

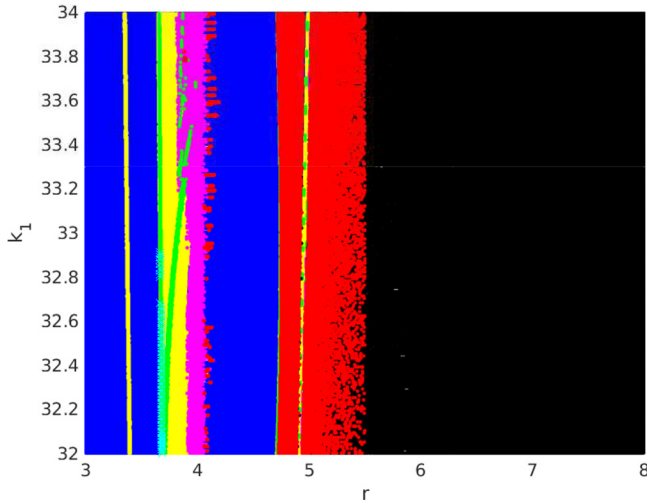


FIG. 4. Choosing  $m = 0.04, g = 140.6, k_2 = 12$  and initial conditions  $(0.05, -0.5, 0.1, -1, 2)$ , regions of various dynamical behaviors for the bifurcation parameters  $r$  and  $k_1$  when both the equilibria  $E_{1,2}$  are asymptotically stable. Periodic regions in blue; Quasi-periodic regions with two zero LEs in yellow; Quasi-periodic regions with three zero LEs in green; Chaos with one zero LEs in purple; Hidden hyperchaotic regions with two positive LEs in red; Hidden hyperchaotic regions with three positive LEs in black.

Fig. 4 shows the regions of various dynamical behaviors in the space of the bifurcation parameters  $(r, k_1) \in [3, 8] \times [32, 34]$  with the other fixed parameters  $m = 0.04, g = 140.6, k_2 = 12$ . To produce Fig. 4, we set  $k_1 = 32$  and incremented  $r$  from 3 to 8. Then we integrated system (2) for 1500 time units to eliminate transients, before beginning to compute the LEs. For the first integration, we took as initial conditions those in Fig. 3. Thereafter, the initial conditions for the next increment in  $r$  were taken to be the final variable values from the previous  $r$ , and the procedure was repeated until  $r = 8$ , when we incremented  $k_1$  to  $k_1 = 32.01$  and began again. Thus a horizontal slice through Fig. 4 at  $k_1 = 34$  should correspond to the middle panel of Fig. 3.

To the best of our knowledge, the phenomenon of multi-stability involving the coexistence of different kinds of

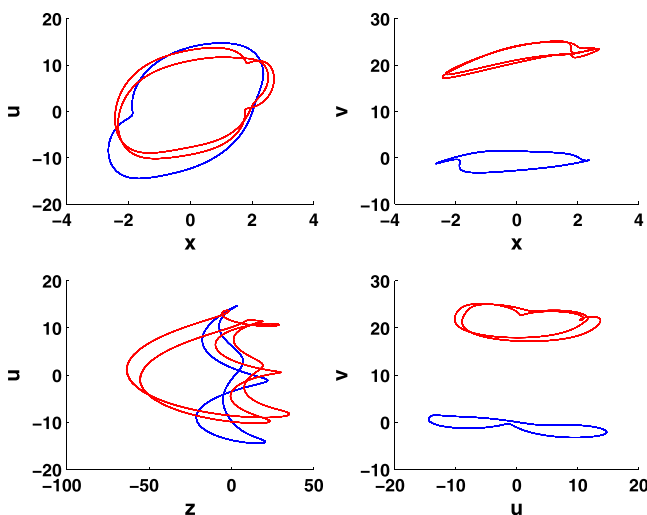


FIG. 5. Coexisting attractors of system (2) with  $r = 3.5$  and  $k_1 = 34$ : period-1 attractor in blue from initial condition  $(2, 1, 2, 0, 0)$ ; period-2 attractor in red from initial condition  $(0, 2, 6, 11, 21)$ .

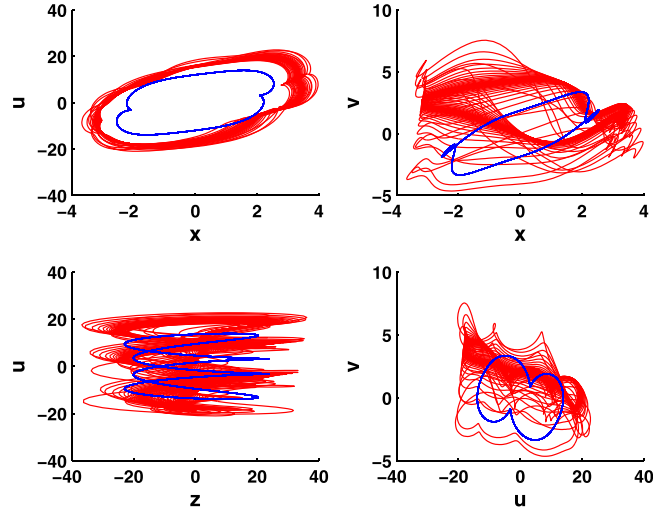


FIG. 6. Coexisting attractors of system (2) with  $r = 2.9$  and  $k_1 = 29.12$ : periodic-1 attractor (blue) from initial condition  $(2, 2, 5, 2, 2)$ ; hidden chaos with LEs  $(0.0628, 0, -0.1497, -0.4999, -1.3133)$  (red) from initial condition  $(2, 0, 1, -4, -2)$ .

hidden attractors with no unstable equilibria has not been reported in higher-dimensional systems (more than 4D), and thus this example is a new contribution to the family of hidden chaotic attractors.

### B. Coexistence of point, periodic, quasi-periodic, and hidden chaotic attractors

Another form of complexity arises when two or more asymptotically stable equilibrium points or attracting sets coexist for a given set of system parameters. For such coexisting attractors, the trajectories of the system selectively converge on one of the attracting sets depending on the initial state of the system.

In the region of parameter space of system (2) where there are two stable equilibria, there can be more than one hidden attractor. Fig. 5 shows an example with  $r = 3.5$  and

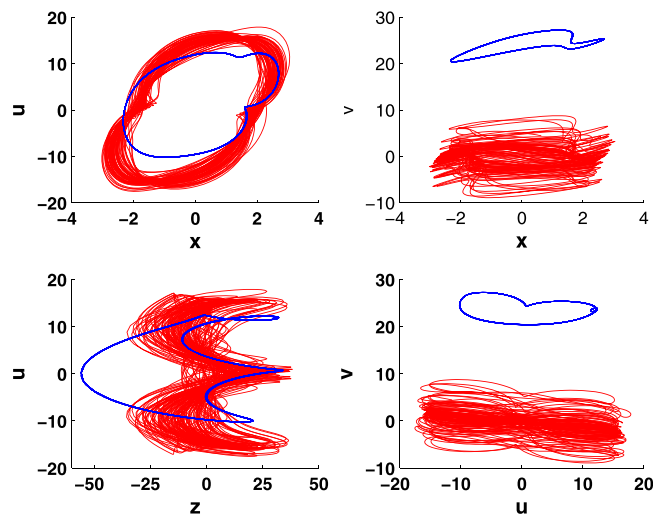


FIG. 7. Coexisting attractors of system (2) with  $r = 3.95$  and  $k_1 = 38$ : periodic-1 attractor (blue) from initial condition  $(0, 2, 6, 11.3, 21)$ ; hidden chaos with LEs  $(0.1635, 0, -0.0450, -0.3909, -2.6776)$  (red) from initial condition  $(0, 2, 6, 11, 2)$ .

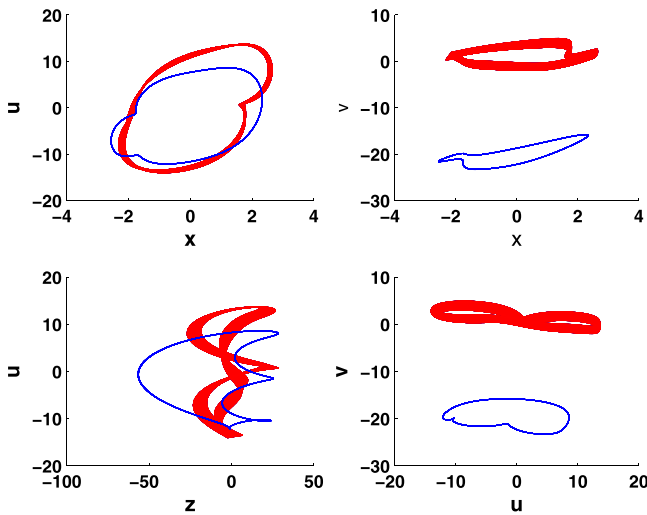


FIG. 8. Coexisting attractors of system (2) with  $r=3.75$  and  $k_1=32$ : periodic-1 attractor (blue) from initial condition (1.5, 4.5, 7.2, 8.5, -19); hidden quasi-periodic orbit with two zero LEs (red) from initial condition (0.05, -0.5, 0.1, -1, 2).

$k_1=34$  where a period-1 and period-2 limit cycle coexist for initial conditions (2, 1, 2, 0, 0) and (0, 2, 6, 11, 21), respectively. Fig. 6 with  $r=2.9$  and  $k_1=29.12$ , and Fig. 7 with  $r=3.95$  and  $k_1=38$  show cases where a limit cycle coexists with a strange attractor. Fig. 8 with  $r=3.75$  and  $k_1=32$  shows a case where a limit cycle coexists with a quasiperiodic attracting torus. Additional evidence that this is a torus rather than a high-period limit cycle or thin strange attractor is provided by Fig. 9 which shows that the cross section of the attractor for  $y=0$  consists of five closed loops. In addition, the Kaplan–Yorke dimension in this region is accurately 2.0.

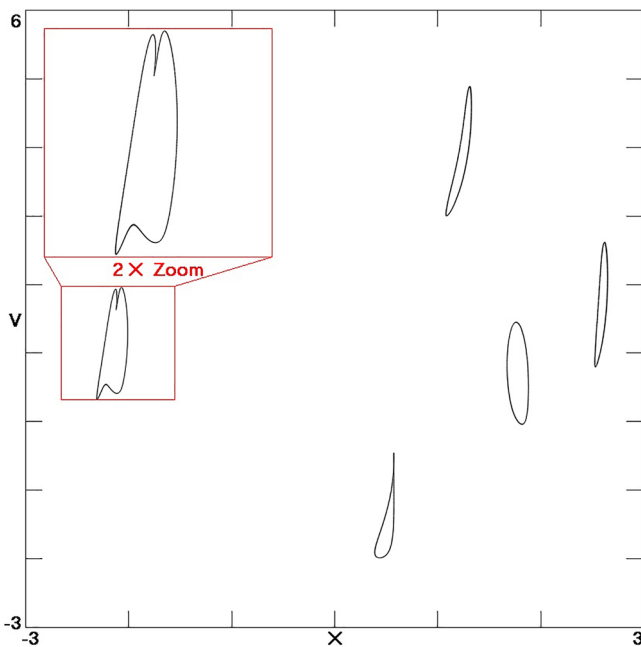


FIG. 9. Quasiperiodic on an attracting torus for cross-section  $y=0$  and parameters  $r=3.75, k_1=32, m=0.04, g=140.6, k_2=12$  of system (2) from initial condition (0.05, -0.5, 0.1, -1, 2).

Whenever there are coexisting attractors, it is useful to examine the basins of attraction. In a 5D system, it is necessary to choose one of the infinitely many planes through the space of initial conditions. A typical case is shown in Fig. 10 where the plane is taken as  $z=20.428, u=6.525x$ , and  $v=300y$  which for the parameters  $r=7, k_1=34, m=0.04, g=140.6, k_2=12$  pass through the two stable equilibria shown as black dots in the figure. Basins of the two symmetric stable equilibria  $E_{1,2}$  are indicated by red and green, respectively, and the basin of the hyperchaotic attractor is in light blue. Two nearby initial conditions in the upper left and lower right of the plot can lead either to the hyperchaotic attractor or to one of the equilibria. This well illustrates why there are long transients in some regions where the basin boundary is extremely complicated.

It is worth noting that coexisting attractors and thus the fractal basin may not be observed in a controlled experiment where system parameters are smoothly varied. In such instances, the initial condition for each parameter value is the final condition (or state) for the previous parameter, and the trajectories are thus locked in only one of the attracting sets.

#### IV. ELECTRONIC CIRCUIT IMPLEMENTATION OF THE 5D HYPERCHAOTIC SYSTEM (2)

Limitations involving components such as analog multipliers and operational amplifiers in electronic circuits require a linear re-scaling of the variables to avoid saturation.<sup>53,54</sup> There is no need to rescale the  $x$  and  $y$  variable values since they fall within the range of  $(-15, 15)$ . However,  $z, u$ , and  $v$  need to be scaled for observations on an oscilloscope. Therefore, we take  $X=x, Y=y, Z=z/10, U=u/5$  and  $V=v/2$  so that system (2) becomes

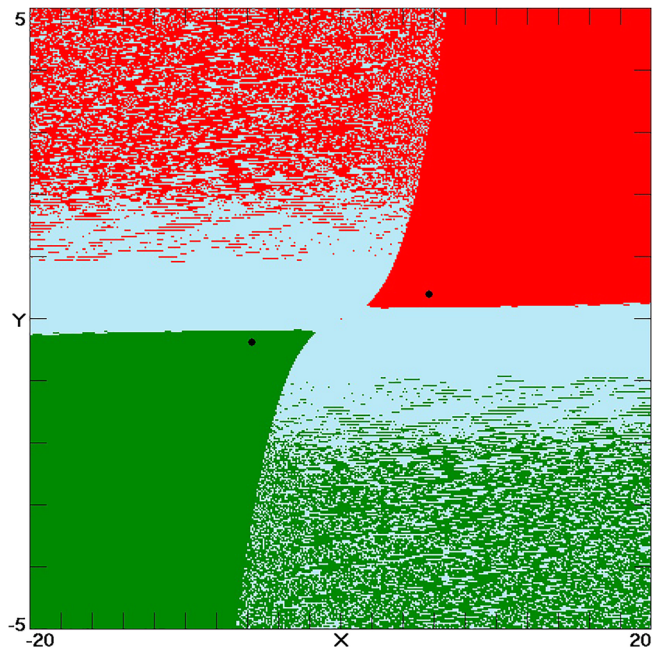


FIG. 10. Cross-section is  $z=20.428, u=6.525x$ , and  $v=300y$  for parameters are  $r=7, k_1=34, m=0.04, g=140.6, k_2=12$ , the light blue is the basin of the hidden hyperchaotic attractors of system (2).

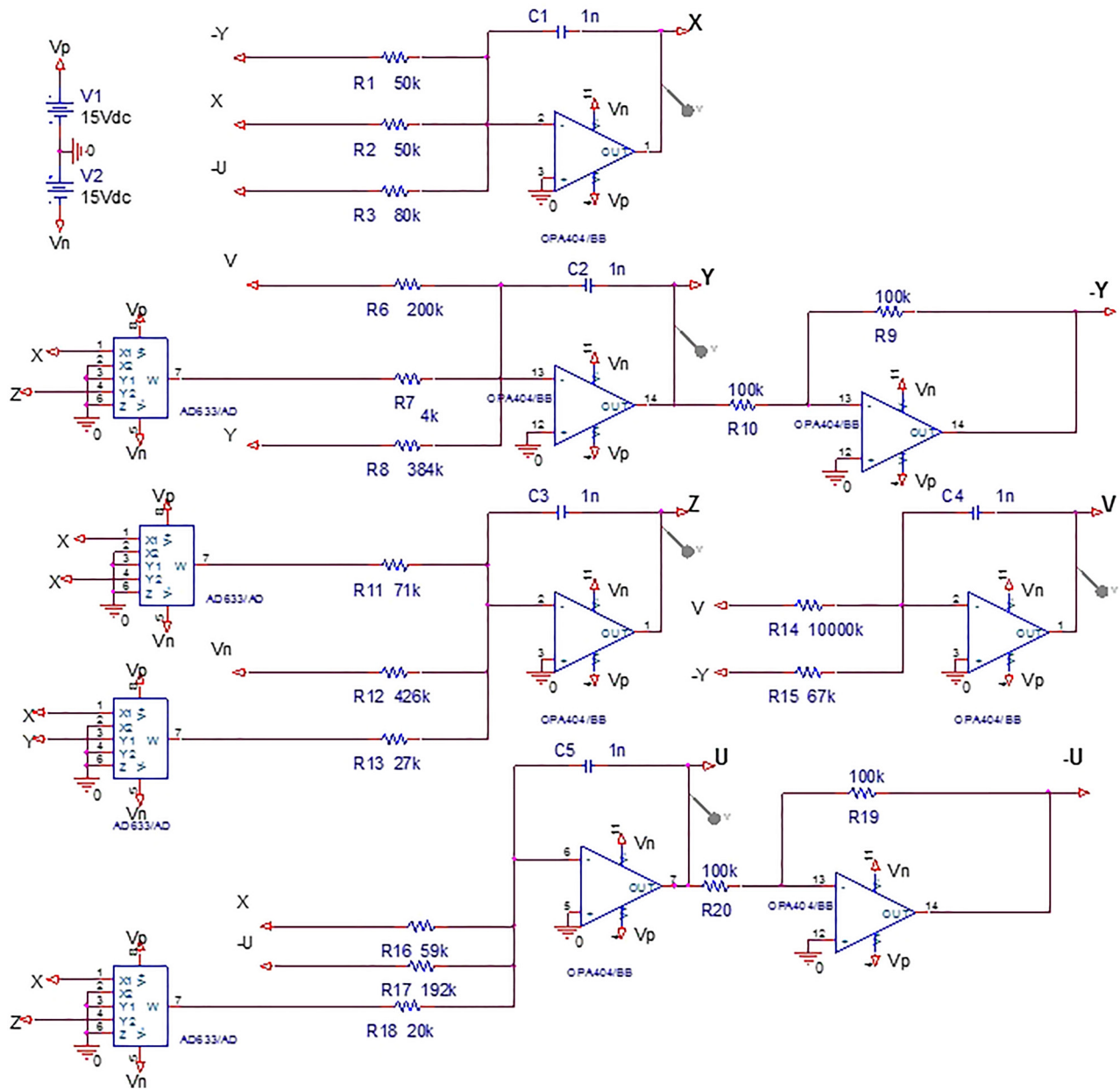


FIG. 11. The electronic circuit schematic of the scaled hyperchaotic system (10) with  $r = 8, m = 0.04, g = 140.6, k_1 = 34, k_2 = 12$ .

$$\begin{cases} \dot{X} = r(Y - X) + 5U, \\ \dot{Y} = -(1 + m)Y + 10XZ - 2V, \\ \dot{Z} = \frac{1}{10}g(1 + mX^2 - (1 + m)XY), \\ \dot{U} = 2(1 + m)U + 2XZ - \frac{1}{5}k_1X, \\ \dot{V} = -mV + \frac{1}{2}k_2Y. \end{cases} \quad (10)$$

In making an electronic circuit exhibiting hidden hyperchaos, one is essentially making an analog computer for system (10). The schematic of the electronic circuit for the rescaled system (10), designed using ORCAD-PSpice, is shown in Fig. 11. The circuit comprises of electronic components such as resistors, capacitors, and operational amplifiers. The electronic circuit for the hyperchaotic system uses

the parameter values of  $r = 8, m = 0.04, g = 140.6, k_1 = 34, k_2 = 12$ , and initial conditions of  $X(0) = 0.05, Y(0) = -0.5, Z(0) = 0.1, U(0) = -1, V(0) = 2$ . The circuit uses TL081 operational amplifiers and AD633 multipliers, with values of  $R_1 = R_2 = 50 \text{ k}\Omega, R_3 = 80 \text{ k}\Omega, R_9 = R_{10} = R_{19} = R_{20} = 100 \text{ k}\Omega, R_6 = 200 \text{ k}\Omega, R_7 = 4 \text{ k}\Omega, R_8 = 384 \text{ k}\Omega, R_{11} = 71 \text{ k}\Omega, R_{12} = 426 \text{ k}\Omega, R_{13} = 27 \text{ k}\Omega, R_{14} = 10 \text{ k}\Omega, R_{15} = 67 \text{ k}\Omega, R_{16} = 59 \text{ k}\Omega, R_{17} = 192 \text{ k}\Omega, R_{18} = 20 \text{ k}\Omega, C_1 = C_2 = C_3 = C_4 = 1 \text{ nF}, V_n = -15 \text{ V}, V_p = 15 \text{ V}$ . The AD633 multiplier IC has inputs in the range of  $-10 \text{ V}$  to  $+10 \text{ V}$ , while the output voltage is a multiple of the input voltage, scaled by  $10 \text{ V}$ . It is tempting to claim that a physical realization provides the real answer to what the system performance is, since it is based on actual physical hardware. A real environmental application of the hyperchaotic system was implemented with electronic components on a breadboard in Fig. 12.



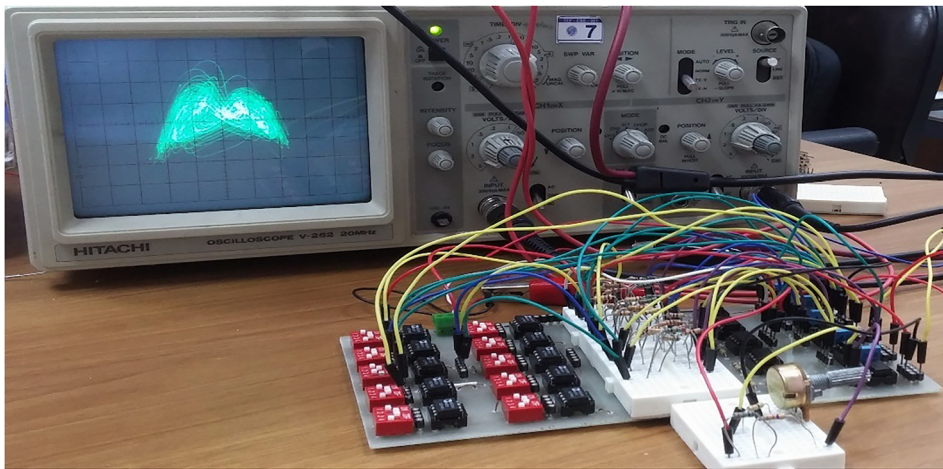


FIG. 12. The experimental circuit of hidden hyperchaos in the scaled hyperchaotic system (10) with  $r=8, m=0.04, g=140.6, k_1=34, k_2=12$ .

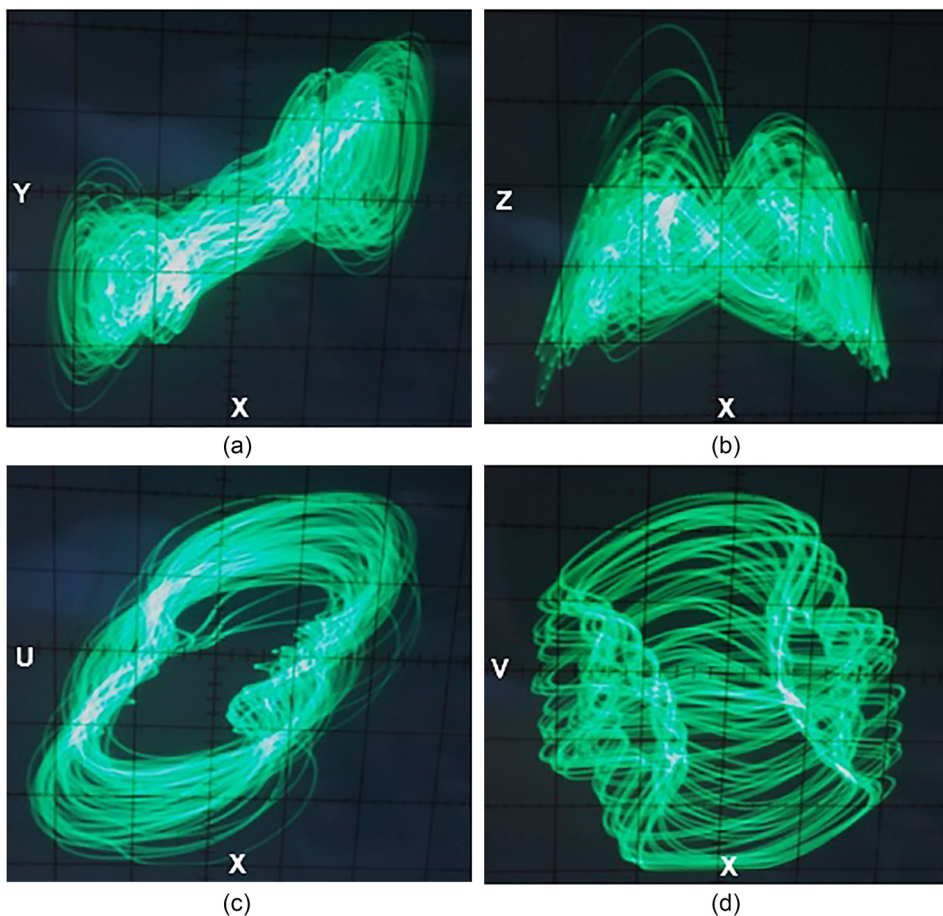


FIG. 13. The phase portraits on the oscilloscope of hidden hyperchaos in the scaled hyperchaotic system (10) with  $r=8, m=0.04, g=140.6, k_1=34, k_2=12$ .

The oscilloscope outputs, showing phase portraits of the rescaled circuit (10) as seen in Fig. 13, agree well with the solution of the equations (2) shown earlier. It is worth noting that the ability to realise the theoretical hidden chaotic attractors plays a very important role in practical applications.<sup>55,56</sup>

## V. CONCLUSION

This paper is a continuation of the study of hidden attractors. A 5D hyperchaotic generalization of a 3D model for a self-exciting homopolar disc dynamo without unstable equilibria but with three positive Lyapunov exponents has been

proposed and investigated. Hidden hyperchaos with only stable equilibria has been observed. The study of such models will lead to further analysis and suggest practical applications of such phenomena. The behaviour presented here shows that complex dynamics can be obtained in 5D systems with only stable equilibria, including periodic attractors (limit cycles), quasi-periodic attractors (tori), chaotic attractors, and hyperchaotic attractors (with two or three positive LEs), all hidden, and suggest that any dynamical phenomenon not explicitly forbidden could in principle feasibly occur. The requirement is to find the right physical example. A future study will elaborate on other aspects of hidden hyperchaos.

## ACKNOWLEDGMENTS

We express our gratitude to Professor H. K. Moffatt for his encouraging comments. We thank the Mathematical Institute, University of Oxford for providing the facilities. This work was supported by the National Natural Science Foundation of China (No. 11401543), the China Scholarship Council (No. 201506415023), the Open Foundation for Guangxi Colleges and Universities Key Lab of Complex System Optimization and Big Data Processing (No. 2016CSOBDP0202), Beijing Postdoctoral Research Foundation (No. 2015ZZ17), the China Postdoctoral Science Foundation funded project (Nos. 2014M560028 and 2015T80029), the Fundamental Research Funds for the Central Universities, China University of Geosciences (Wuhan) (No. CUGL150419), the Government of Chaoyang District Postdoctoral Research Foundation (No. 2015ZZ-7), and Sakarya University Scientific Research Projects Unit (No. 201609-00-008).

- <sup>1</sup>J. C. Sprott, "Some simple chaotic flows," *Phys. Rev. E* **50**, R647–650 (1994).
- <sup>2</sup>D. Dudkowski, S. Jafari, T. Kapitaniak, N. V. Kuznetsov, G. A. Leonov, and A. Prasad, "Hidden attractors in dynamical systems," *Phys. Rep.* **637**, 1–50 (2016).
- <sup>3</sup>H. K. Moffatt, "A self consistent treatment of simple dynamo systems," *Geophys. Astrophys. Fluid Dyn.* **14**, 147–166 (1979).
- <sup>4</sup>Y. M. Chen and Q. G. Yang, "Dynamics of a hyperchaotic Lorenz-type system," *Nonlinear Dyn.* **77**, 569–581 (2014).
- <sup>5</sup>R. Barrio, M. A. Martínez, S. Serrano, and D. Wilczak, "When chaos meets hyperchaos: 4D Rössler model," *Phys. Lett. A* **379**(38), 2300–2305 (2015).
- <sup>6</sup>R. Chertovskih, E. V. Chimanski, and E. L. Rempel, "Route to hyperchaos in Rayleigh-Bénard convection," *Europhys Lett.* **112**, 14001 (2015).
- <sup>7</sup>Z. L. Wang, L. L. Zhou, Z. Q. Chen, and J. Z. Wang, "Local bifurcation analysis and topological horseshoe of a 4D hyper-chaotic system," *Nonlinear Dyn.* **83**, 2055–2066 (2016).
- <sup>8</sup>G. Hu, "Generating hyperchaotic attractors with three positive Lyapunov exponents via state feedback control," *Int. J. Bifurcation Chaos* **19**, 651–660 (2009).
- <sup>9</sup>Q. G. Yang and C. Chen, "A 5D hyperchaotic system with three positive Lyapunov exponents coined," *Int. J. Bifurcation Chaos* **23**, 1350109 (2013).
- <sup>10</sup>P. C. Rech, "Delimiting hyperchaotic regions in parameter planes of a 5D continuous-time dynamical system," *Appl. Math. Comput.* **247**(15), 13–17 (2014).
- <sup>11</sup>Q. G. Yang, W. M. Osman, and C. Chen, "A new 6D hyperchaotic system with four positive Lyapunov exponents coined," *Int. J. Bifurcation Chaos* **25**, 1550060 (2015).
- <sup>12</sup>L. P. Sil'nikov, "A contribution to the problem of the structure of an extended neighborhood of a rough equilibrium state of saddle-focus type," *Math. USSR-Shornik* **10**, 91–102 (1970).
- <sup>13</sup>C. P. Silva, "Shil'nikov's theorem—a tutorial," *IEEE Trans. Circuits Syst. I* **40**(10), 657–682 (1993).
- <sup>14</sup>J. C. Sprott, "Strange attractors with various equilibrium types," *Eur. Phys. J.: Spec. Top.* **224**, 1409–1419 (2015).
- <sup>15</sup>D. Dudkowski, A. Prasad, and T. Kapitaniak, "Perpetual points and periodic perpetual loci in maps," *Chaos* **26**, 103103 (2016).
- <sup>16</sup>N. V. Kuznetsov, G. A. Leonov, and S. M. Seledzhi, "Hidden oscillations in nonlinear control systems," *IFAC Proc. Vol.* **44**, 2506–2510 (2011).
- <sup>17</sup>N. V. Kuznetsov, O. A. Kuznetsov, G. A. Leonov, and V. I. Vagaitsev, "Hidden attractor in Chua's circuits," in *ICINCO 2011 - Proceedings of the 8th International Conference on Informatics in Control, Automation and Robotics* (2011), pp. 27–283.
- <sup>18</sup>G. A. Leonov, N. V. Kuznetsov, and V. I. Vagaitsev, "Localization of hidden Chua's attractors," *Phys. Lett. A* **375**(23), 2230–2233 (2011).
- <sup>19</sup>G. Leonov, N. Kuznetsov, and V. Vagaitsev, "Hidden attractor in smooth Chua systems," *Physica D* **241**(18), 1482–1486 (2012).
- <sup>20</sup>G. A. Leonov and N. V. Kuznetsov, "Hidden attractors in dynamical systems. From hidden oscillations in Hilbert-Kolmogorov, Aizerman, and Kalman problems to hidden chaotic attractor in Chua circuits," *Int. J. Bifurcation Chaos* **23**(1), 1330002 (2013).
- <sup>21</sup>G. A. Leonov, N. V. Kuznetsov, and T. N. Mokaev, "Hidden attractor and homoclinic orbit in Lorenz-like system describing convective fluid motion in rotating cavity," *Commun. Nonlinear Sci. Numer. Simul.* **28**(1–3), 166–174 (2015).
- <sup>22</sup>D. Dudkowski, A. Prasad, and T. Kapitaniak, "Perpetual points and periodic perpetual loci in maps," *Phys. Lett. A* **379**(40–41), 2591–2596 (2015).
- <sup>23</sup>T. Kapitaniak and G. A. Leonov, "Multistability: Uncovering hidden attractors," *Eur. Phys. J.: Spec. Top.* **224**, 1405–1408 (2015).
- <sup>24</sup>Z. C. Wei, "Dynamical behaviors of a chaotic system with no equilibria," *Phys. Lett. A* **376**, 102–108 (2011).
- <sup>25</sup>Z. Wang, S. Cang, E. O. Ochola, and Y. Sun, "A hyperchaotic system without equilibrium," *Nonlinear Dyn.* **69**, 531–537 (2012).
- <sup>26</sup>S. Jafari, J. C. Sprott, and S. Golpayegani, "Elementary quadratic chaotic flows with no equilibria," *Phys. Lett. A* **377**, 699–702 (2013).
- <sup>27</sup>V. T. Pham, C. Volos, and L. V. Gambuzza, "A memristive hyperchaotic system without equilibrium," *Sci. World J.* **2014**, 1–9.
- <sup>28</sup>Z. C. Wei, R. Wang, and A. P. Liu, "A new finding of the existence of hidden hyperchaotic attractors with no equilibria," *Math. Comput. Simul.* **100**, 13–23 (2014).
- <sup>29</sup>Z. C. Wei, J. C. Sprott, and H. Chen, "Elementary quadratic chaotic flows with a single non-hyperbolic equilibrium," *Phys. Lett. A* **379**, 2184–2187 (2015).
- <sup>30</sup>Q. G. Yang, Z. C. Wei, and G. Chen, "An unusual 3D autonomous quadratic chaotic system with two stable node-foci," *Int. J. Bifurcation Chaos* **20**, 1061–1083 (2010).
- <sup>31</sup>X. Wang and G. Chen, "A chaotic system with only one stable equilibrium," *Commun. Nonlinear Sci. Numer. Simul.* **17**, 1264–1272 (2012).
- <sup>32</sup>M. Molaie, S. Jafari, J. C. Sprott, and S. Mohammad, "Simple chaotic flows with one stable equilibrium," *Int. J. Bifurcation Chaos* **23**, 1350188 (2013).
- <sup>33</sup>G. A. Leonov, N. V. Kuznetsov, and T. N. Mokaev, "Homoclinic orbits, and self-excited and hidden attractors in a Lorenz-like system describing convective fluid motion," *Eur. Phys. J.: Spec. Top.* **224**(8), 1421–1458 (2015).
- <sup>34</sup>Q. D. Li, H. Z. Zeng, and J. Li, "Hyperchaos in a 4D memristive circuit with infinitely many stable equilibria," *Nonlinear Dyn.* **79**(4), 2295–2308 (2015).
- <sup>35</sup>B. C. Bao, Q. D. Li, N. Wang, and Q. Xu, "Multistability in Chua's circuit with two stable node-foci," *Chaos* **26**, 043111 (2016).
- <sup>36</sup>Z. C. Wei and W. Zhang, "Hidden hyperchaotic attractors in a modified Lorenz-Stenflo system with only one stable equilibrium," *Int. J. Bifurcation Chaos* **24**, 1450127 (2014).
- <sup>37</sup>Z. C. Wei, P. Yu, W. Zhang, and M. H. Yao, "Study of hidden attractors, multiple limit cycles from Hopf bifurcation and boundedness of motion in the generalized hyperchaotic Rabinovich system," *Nonlinear Dyn.* **82**, 131–141 (2015).
- <sup>38</sup>S. Jafari and J. C. Sprott, "Simple chaotic flows with a line equilibrium," *Chaos, Solitons Fractals* **57**, 79–84 (2013).
- <sup>39</sup>Q. D. Li, S. Y. Hu, S. Tang, and G. Zeng, "Hyperchaos and horseshoe in a 4D memristive system with a line of equilibria and its implementation," *Int. J. Circuit Theory Appl.* **42**(11), 1172–1188 (2014).
- <sup>40</sup>J. C. Sprott, X. Wang, and G. Chen, "Coexistence of point, periodic and strange attractors," *Int. J. Bifurcation Chaos* **23**(5), 1350093 (2013).
- <sup>41</sup>C. Li and J. C. Sprott, "Coexisting hidden attractors in a 4-D simplified Lorenz system," *Int. J. Bifurcation Chaos* **24**(3), 1450034 (2014).
- <sup>42</sup>M. Chen, J. J. Yu, and B. C. Bao, "Finding hidden attractors in an improved memristor based Chua's circuit," *Electron. Lett.* **51**(6), 462–464 (2015).
- <sup>43</sup>N. V. Kuznetsov and G. A. Leonov, "Numerical Visualization of attractors: Self-exciting and hidden attractors," in *Handbook of Applications of Chaos Theory* (2016), pp. 135–143.
- <sup>44</sup>S. T. Kingni, S. Jafari, V. T. Pham, and P. Wofo, "Constructing and analyzing of a unique three-dimensional chaotic autonomous system exhibiting three families of hidden attractors," *Math. Comput. Simul.* **132**, 172–182 (2017).
- <sup>45</sup>E. Knobloch, "Chaos in the segmented disc dynamo," *Phys. Lett. A* **82**, 439–440 (1981).
- <sup>46</sup>R. Hide, A. C. Skeldon, and D. J. Acheson, "A study of two novel self-exciting single-disk homopolar dynamos: Theory," *Proc. R. Soc. London, Ser. A* **452**, 1369–1395 (1996).

- <sup>47</sup>I. M. Moroz, R. Hide, and A. M. Soward, "On self-exciting coupled Faraday disk homopolar dynamos driving series motors," *Physica D* **117**, 128–144 (1998).
- <sup>48</sup>A. Wolf, J. B. Swift, H. L. Swinney, and J. A. Vastano, "Determining Lyapunov exponents from a time series," *Physica D* **16**, 285–317 (1985).
- <sup>49</sup>G. A. Leonov and N. V. Kuznetsov, "Time-varying linearization and the Perron effects," *Int. J. Bifurcation Chaos* **17**, 1079–1107 (2007).
- <sup>50</sup>V. N. Govorukhin, see <http://kvm.math.rsu.ru/matds/> for MATDS (2004).
- <sup>51</sup>N. V. Kuznetsov, G. A. Leonov, and T. N. Mokaev, "The Lyapunov dimension and its computation for self-excited and hidden attractors in the Glukhovskiy-Dolzhansky fluid convection model," preprint [arXiv:1509.09161v2](https://arxiv.org/abs/1509.09161v2) (2016).
- <sup>52</sup>N. V. Kuznetsov, T. A. Alexeeva, and G. A. Leonov, "Invariance of Lyapunov exponents and Lyapunov dimension for regular and irregular linearizations," *Nonlinear Dyn.* **85**(1), 195–201 (2016).
- <sup>53</sup>A. Akgul, I. Moroz, I. Pehlivan, and V. Sundarapandian, "A new four-scroll chaotic attractor and its engineering applications," *Optik - Int. J. Light Electron Opt.* **127**(13), 5491–5499 (2016).
- <sup>54</sup>A. Akgul, H. Shafqat, and I. Pehlivan, "A new three-dimensional chaotic system, its dynamical analysis and electronic circuit applications," *Optik - Int. J. Light Electron Opt.* **127**(18), 7062–7071 (2016).
- <sup>55</sup>G. Bianchi, N. V. Kuznetsov, G. A. Leonov, S. M. Seledzhi, M. V. Yuldashev, and R. V. Yuldashev, "Hidden oscillations in SPICE simulation of two-phase Costas loop with non-linear VCO," *IFAC-PapersOnLine* **49**(14), 45–50 (2016).
- <sup>56</sup>G. Bianchi, N. V. Kuznetsov, G. A. Leonov, M. V. Yuldashev, and R. V. Yuldashev, "Limitations of PLL simulation: hidden oscillations in MATLAB and SPICE," in *Proceedings of the IEEE 7th International Congress on Ultra Modern Telecommunications and Control Systems Workshops (ICUMT)* (2015), pp. 79–84.